PAPER

Reconfigurable laminates enable multifunctional robotic building blocks

To cite this article: Mingsong Jiang and Nicholas Gravish 2021 *Smart Mater. Struct.* **30** 035005

View the article online for updates and enhancements.

Reconfigurable laminates enable multifunctional robotic building blocks

Mingsong Jiang® and **Nicholas Gravish**®

Department of Mechanical and Aerospace Engineering, University of California, San Diego, United States of America

E-mail: ngravish@eng.ucsd.edu

Abstract

Folding and assembling of two-dimensional laminated materials have greatly facilitated robot fabrication by creating robots with lightweight body frames, articulated joints, and embedded actuators and sensors. The combinations of rigid laminates bridged by thin-film flexures, often called rigid-flex linkages, have been extensively used in micro- and macro-scale robots to achieve complex joint motions with simplified kinematic and dynamic properties. Much like traditional robots these rigid-flex laminate robots are designed with a fixed body-plan, and thus may face challenges when environments require mechanical reconfiguration such as stiffening joints for load support or changing appendage morphologies for navigating confined spaces. Recent advances in adaptive materials and smart actuators have highlighted the features that robots with morphable geometries and tunable mechanical properties can provide, such as self-folding joints and variable stiffness and damping mechanisms. However, incorporation of these reconfigurable elements into laminate robots has been limited. In this paper, we present a new method for creating quasi two-dimensional structures for robotics, called reconfigurable laminates, that use geometric reconfiguration of laminate layers to alter passive mechanical properties and actuate joints. Unlike traditional rigid-flex linkages with single-layered flexures, here we create laminate joints with dual-layered soft hinges and rigid channels allowing a multitude of reconfiguration opportunities including: sliding-layer laminates for passive stiffness control, snapping-hinge locks for reconfigurable joints, and buckle-bend joints for bending actuation. Through experimental characterization we demonstrate the capabilities of these multifunctional robotic building blocks.

Supplementary material for this article is available online

Keywords: reconfigurable laminates, laminate robots, variable stiffness, planar fabrication

(Some figures may appear in colour only in the online journal)

1. Introduction

Incorporation of reconfigurable mechanisms in robot design can enable multi-functional capabilities in various and changing working conditions [1–4]. When needed, a reconfigurable robot can adjust either its partial or entire body structure to exhibit different kinematic or mechanical properties such as transformable shapes [5, 6] and locomotion [7] with tunable stiffness [8] or damping [9] to meet with changed environments. Such designs and mechanisms grant robots the ability to switch between different locomotion modes or even generate new behaviors to suit complex environments that may not be easily accessed from a pure control or learning process [10–12]. For instance, a flapping-wing robot will be more versatile and energy-efficient to have tunable hinge stiffness when facing changing fluidic conditions; meanwhile, a swimming robot will be unlikely to navigate through a confined tunnel without shrinking its body size as well as adjusting its tail locomotion. However, it should be noted that the benefits from using reconfigurable mechanisms might be counteracted

by factors such as extra energy consumption for maintaining a reconfigured state [13] or actuation mechanisms (such as thermal [14], electric [15] and magnetic fields [16]) that may limit operation environments. Instead, by borrowing the concept of material reinforcement from laminate composites and incorporating the ability to reconfigure laminate arrangement, one may achieve tunable material properties based on internal geometric layouts instead of material adaptivity activated by external stimuli [17, 18]. In this paper, we explore the design opportunities and capabilities of reconfigurable laminates by creating multiple types of reconfigurable laminate structures based on planar robot fabrication methods that are easily embeddable as multi-functional robotic building blocks.

Robots built from folding and assembling of two-dimensional laminated materials, such as smart composite microstructure (SCM) [19, 20], provide convenient and rapid fabrication capabilities for a range of robot scales and applications [21–23]. Such a design paradigm stems from traditional microelectromechanical systems (MEMS) manufacturing [24, 25] by constructing three-dimensional robot components using layered materials and structures. The method achieves multi-material composites based on laser (micro-)machining and lamination processes, which can be manually folded and assembled into functional parts, such as robot frameworks [26, 27], joints [28, 29] and appendages [30, 31]. Based on this technology, a library of mobile [22, 32, 33] and surgical robots [34, 35] with articulated microstructures were made possible in ever smaller scales (μm–mm). Such an enabling fabrication technique was also adapted to rapidly prototype macroscale (cm and larger) robot systems with onboard controls [36, 37].

Meanwhile, fabrication of an SCM laminate robot can require intensive manual labor involving layer alignment, discrete component assembly, and multiple cut and cure steps [38]. To alleviate the assembly process, researchers have developed novel design and fabrication tools inspired by pop-up children's books [22, 39] or foldable origami [29, 40]. Despite the vast improvements to laminate robot fabrication, the overarching design paradigm remains unchanged. Laminate robots are designed with rigid linkages bridged by flexible hinges, often called rigid-flex linkages [39], that are interconnected in a fixed body-plan, and actuated with rigid mechanisms such as four-bar linkages [19, 41]. The rigid-flex paradigm of laminate joint design means that laminate robots suffer from the same challenges as traditional robots composed of rigid links and actuated joints, namely a lack of kinematic or mechanical reconfigurability and adaptability to novel or unexpected working conditions. For instance, a flying robot with constant hinge stiffness might not generate enough lift forces with a low amplitude flapping mode or increased payloads, whereas a crawling robot could be stuck outside a confined tunnel with an incompressible body frame.

Alternatively, soft robots composed of highly deformable materials are enabling new capabilities for robots to interact with challenging environments through material compliance and geometric reconfigurability [42, 43]. However, robots made from inherently soft materials (generally, Young's Modulus < 10 Mpa) may lack the ability to generate significant forces against their environment. Such dynamic range in force generation may be necessary for locomotion and interaction tasks [44, 45], such as conforming around external obstacles (softness) and then anchoring onto walls (rigidity). Methods such as pneumatically induced particle and layer jamming have been provided for stiffening soft body frames [46, 47]; however, they often require the target systems to be tethered with a powerful pressure generator (either positive or negative) which might seem cumbersome for mobile robot applications. Recent advances in smart materials and actuators have been implemented to solve the problem by incorporating active materials inside the soft hinged regions as low-profile robot modulations [48, 49]. Examples such as dielectric laminates with low-melting point alloy to achieve variable stiffness bending structures [13] as well as shape memory polymers to enable self-folding mechanisms based on thermal activations [14, 50] have all been demonstrated to vary the mechanical properties of the laminate robots to some extent. However, such methods are highly dependent on the use of external control signals or specific environmental settings that might not be suitable for energy conservative robot applications. Therefore, it is of high importance to achieve reconfigurable robot kinematic and mechanical properties that are passively stable with embeddable activation approaches.

Laminate structures present an opportunity for the design of such reconfigurable robots. By allowing layers within a laminate to move relative to each other, the configuration of regions with different mechanical properties, or actuation and sensing capabilities, can be controlled to provide mechanical reconfiguration. In this paper we present a new design paradigm for adaptive laminate robots called reconfigurable laminates that use dissimilar laminated layers capable of translating in-plane with respect to each other to tune mechanical properties, reconfigure joint locations, and actuate. By laminating traditional rigid-flex linkages in a dual-layered fashion, inter-layer sliding motions as well as hinge buckling and snapping motions can be formed. Mechanical properties such as bending stiffness and lockable joints can be controlled based on the changeable alignment states between the rigid and soft components as well as the hysteretic buckling and snap through from the soft layered regions. The same units can also be actuated to create rotary joint motions with low-profile tendon actuation. This paper is arranged as follows. We begin with the introduction of three exemplary reconfigurable laminates: variable stiffness sliding-layer laminates, reconfigurable joints with bi-stable layer snapping, and joint actuators from buckle-bend mechanisms. These reconfigurable laminate designs are all fabricated through the common SCM process and thus can be readily incorporated into laminate robots. Each mechanism is further studied based on different design parameters to capture a broader spectrum of tunable mechanical properties. To inspire the use of reconfigurable laminates we present a gallery of multifunctional mechanisms for a variety types of robotic designs and applications.
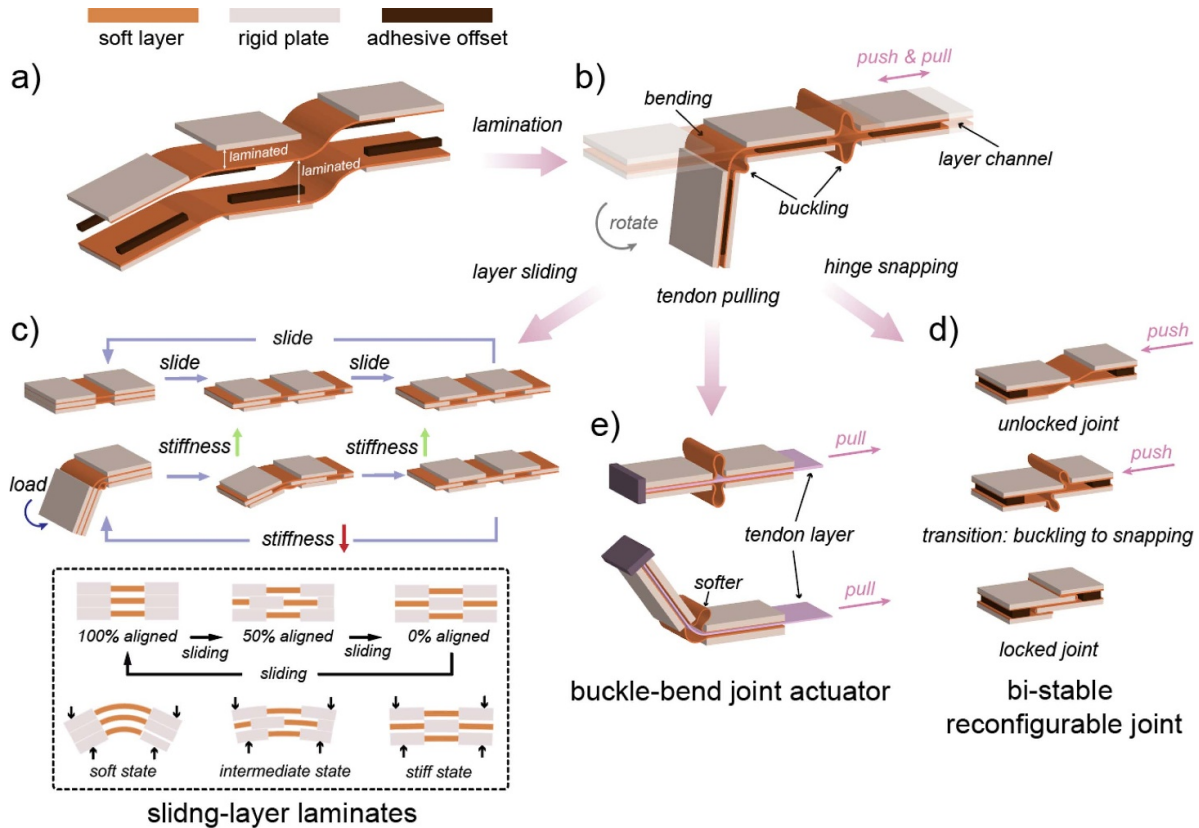
Figure 1. Design overview and three embodiments of reconfigurable laminates. (a) An exploded view showing the material composition of a fundamental dual-layered reconfigurable laminate unit. Thin polyimide sheets (soft layers) and fiberglass sheets (rigid plates) were laminated to create a single laminate layer. Rigid bonding offsets are inserted in between to form internal layer channels. (b) Soft hinged regions are capable of bending and buckling based on external load conditions. This creates the geometric reconfigurations needed for tunable kinematic and mechanical properties. (c) Sliding-layer laminates with different layer alignment to achieve tunable passive bending stiffness. Bottom: a schematic showing the details of the functioning of the sliding layer mechanism. (d) A bi-stable reconfigurable joint created from buckling and snap-through of the offsetted soft layers under external translational forces. The locked state is passively stable due to interlayer surface frictions. (e) A joint actuator enabled by tendon pulling which causes either joint contraction or bending based on either symmetric or asymmetric buckling from the soft regions. (f) A schematic diagram showing the functioning of the stiffness patterns and the layer channels that can be reconfigured to generate tunable material properties.

2. Conceptual design

Reconfigurable laminates take on many forms based on specific laminate designs and material layouts. However, the common design of reconfigurable laminates is to utilize different geometric configurations of the constituent rigid and soft components leading to tunable kinematic and mechanical properties. Such reconfigurability is made possible via the creation of dual-layered soft hinges and rigidly supported layer channels allowing either interlayer sliding or internal joint hinge snapping motion. Here we introduce the fundamental material composition of a reconfigurable laminate unit. To start with, an upper and a lower layer with a periodic rigid-flex array are adhered together with vertical bonding offsets to form an empty layer channel in the middle of the sandwiched structure (figures 1(a) and (b)). For the soft layers we used flexible yet inextensible thin polyimide films (Kapton, 0.02–0.1 mm) and reinforcement composites such as fiberglass (FR-4, 0.12–0.5 mm) for the rigid plates as shown in figure 1(a). Once the outer frame of the reconfigurable laminate is formed, we are able to deform the soft hinged regions

in either bending or buckling modes based on external load conditions (figure 1(b)) or through the use of internal sliding-layers (figures 1(c) and (e)). By tailoring the design of the outer and central layers, we create laminates that function as variable stiffness elements (figure 1(c)), reconfigurable joints (figure 1(d)), joint actuators (figure 1(e)). Here we design these three functionalities and motivate the design choices that enable them.

2.1. Variable stiffness sliding-layer laminates

Variable stiffness materials can be created through geometric reconfigurations of the constituent rigid and soft components. As shown in figure 1(c), a central layer with the same stiffness patterns is slid with regard to the outer layers to form different layer alignments of the dissimilar material components. The outer layers are kept bonded during the sliding motion using high bond strength adhesives (3 M, polyester plastic mounting tape) where the sliding interface is covered with polyimide films (Kapton, 0.025–0.05 mm) to further reduce interlayer jamming issues. When rigid regions of the central

layer overlap with the outer flexible regions, the entire structure becomes stiff. As the layer alignment keeps shifting, soft hinges will be exposed whose bending stiffness can be tuned based on the ongoing layer alignments. A schematic has been shown (figure 1(c) bottom) for better understanding of the sliding mechanism. The layer alignment states are labeled as a percentage where a 0% aligned state means complete misalignment (central layer's rigid plates facing the soft hinges of the outer laminates). Multiple sliding-layer laminate units can be put in series for modulating the mechanical property of an entire continuum structure with a single central laminate layer. It will be shown that incorporating multi-axis sliding motion and stiffness patterns will lead to stiffness control of laminate structures in multiple directions.

2.2. Bi-stable reconfigurable joint

In addition to bending, hysteretic behaviors such as layer buckling can be exploited to build bi-stable reconfigurable joints that passively hold either a flexible or locked state. Such a mechanism is demonstrated by exerting forces onto a laminate joint with offsetted soft hinges capable of buckling and snapping inside the confined layer channels (figure 1(d)). The joint can thus be locked by interlayer surface friction with adjacent rigid plates overlapping with each other to form an increased bending stiffness. Such a mechanism can be applied for discrete stiffness and motion control (locking/unlocking) at specific joint locations, as opposed to the sliding-layer mechanism, where the stiffness of the entire bending structure is uniformly changed. The intrinsic bistability of the buckled film makes the reconfigured joints passively stable in the locked state.

2.3. Buckle-bend joint actuator

Replacing the central laminate with a uniform tendon layer can induce bending actuation of the flexible joints. To actuate a laminate joint, a tendon layer is displaced with jammable features by the far end of one laminate unit, which induces buckling of the soft hinge by pulling on the tendon (figure 1(e)). Depending on the material properties of the buckling regions, either beam contraction or directional bending can be observed due to the corresponding buckling states of the soft layers. One unique aspect of this design is that directional bending of the joint is not induced from an offset tendon lever arm, as mostly seen in tendon-driven robot applications [51], but instead through the asymmetry of the outer layer flexibility. One benefit of such designs is they enable low-profile, easily embeddable laminated joint structures that can also be combined with other reconfigurable modules for multi-functional bending actuators.

The rest of the paper explains the fabrications and the results from different types of experiments showing the variously tunable material properties by using simple actuation methods. For our testing, most of the laminate reconfigurations were achieved via motorized linear actuators or hands on demonstrations; however, for implementation of these materials into robots, we envision many different actuation methods can be applied, such as tendon-driven actuators [51, 52], smart materials (e.g. SMAs [53] and LCEs [54]), and magnets (or magnetic coating) [2, 55] incorporated into the layers will then be actuated remotely by external magnetic fields. Integrating these actuation methods within the SLL structures is an exciting future area of work for reconfigurable robotics.

3. Materials and methods

Fabrication of reconfigurable laminates is based on a modification of SCM manufacturing [19]. For ease of mechanism observations, experimental samples and prototypes are usually made at the macro-scale (mm-cm), where we used flexible and inextensible polymeric sheets such as polyimide (Kapton, HN, 0.025–0.075 mm thickness) and polyester (Mylar, 0.025–0.1 mm thickness) to form the soft regions with the rigid regions composed by fiberglass composites (FR-4, 0.12–0.5 mm). We used off-the-shelf laser cutting (Glowforge) for creating individual layer stiffness patterns. Individual layers were bonded based on double-sided adhesive films (3 M, No. 82600, 5 μm) which were manually aligned and adhered under pressure (Carver, No. 4120) into laminated structures. A general procedure for fabricating the laminated reconfigurable building blocks is described as follows.

To build reconfigurable laminates, we start with laser cutting individual layers (both rigid and soft) which are usually pre-bonded with double-sided adhesives to eliminate unnecessary extra cuts (figure 2(a)). Individual layers after cutting are manually aligned and laminated using a hydraulic press (2000–5000 psi for 10–30 s). Extra support material is thus cut away in the laser to form a single piece of laminate layer with pre-designed stiffness patterns (figure 2(a)). To form a sliding layer channel for the central laminate, the outer laminate layers are bonded by rigid offsets with adhesives coated on the contact surfaces. The rigid offsets are made of fiberglass strips (FR-4, 0.12–0.5 mm) coated with double-sided adhesives (3 M, polyester plastic mounting tape). The offsets are only applied on the rigid plates where the top and bottom layers are aligned and further bonded at a lower pressure (1000–2000 psi for 1 min). The whole purpose for the rigid offsets is to form a sliding layer channel allowing the central laminate layer to move freely without causing damage to the whole structure. Thus, sliding layer laminates should be able to repeatedly switch between their stiff and soft states for continual use. A central laminate with the same stiffness patterns can be inserted after the lamination of the outer laminate structure to generate the prescribed variable passive bending stiffness as shown in figure 2(a). Note that Kapton films were used to cover all sliding surfaces to create a smooth interlayer sliding interface. In figure 2(b) we demonstrate three different states of a sliding-layer laminate prototype, which are: flexible individual laminate layers that are separated, soft and stiff
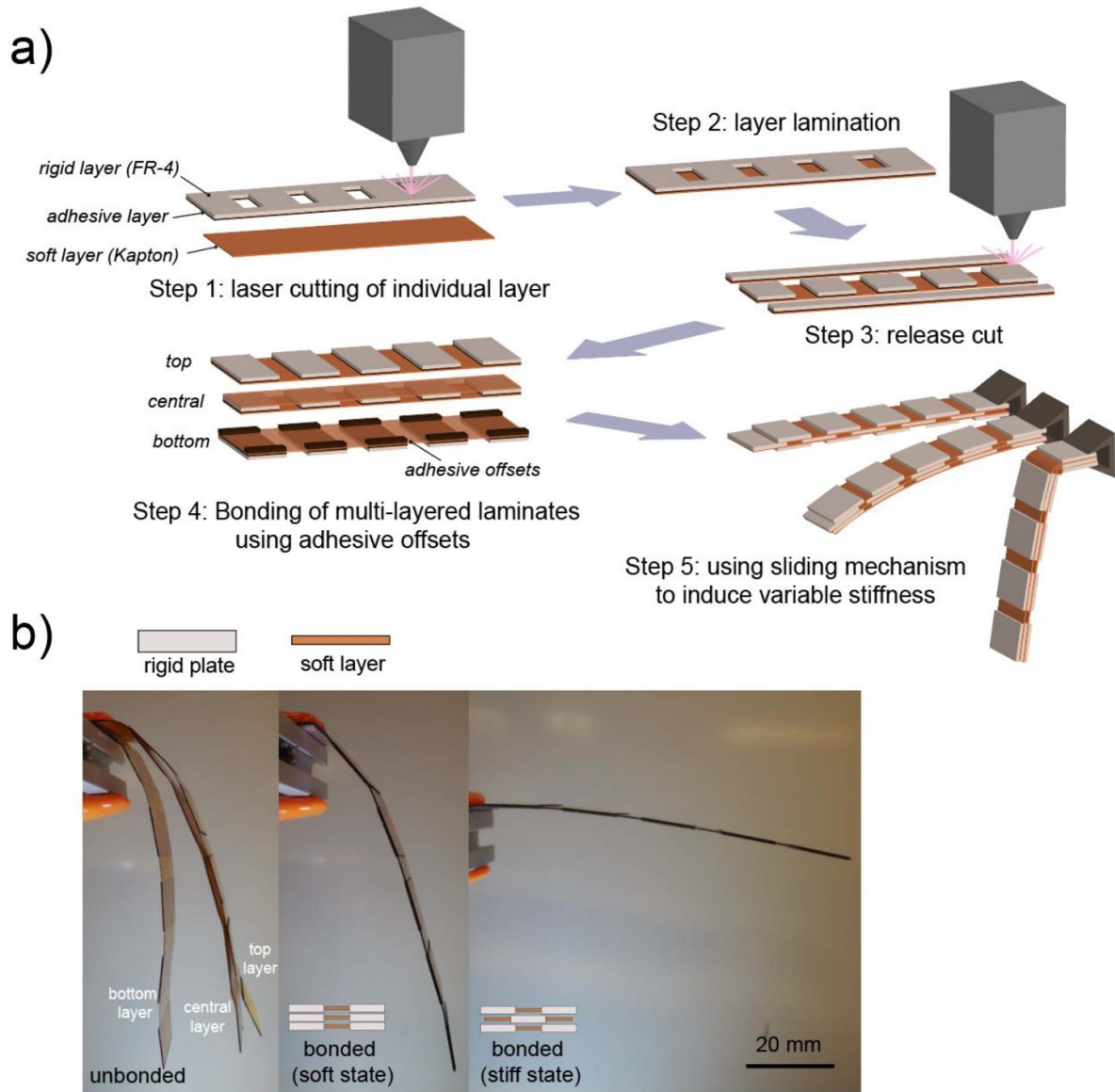
Figure 2. Fabrication of reconfigurable laminates. (a) General process for making reconfigurable laminate designs. Note that the process is applicable for building all types of reconfigurable laminate designs and that the material choices can range from cuttable sheets of metals, fibers, and plastics to create desired tunable material properties. (b) Demonstrations of sliding-layer laminates with unboned individual laminates and bonded laminates in soft (aligned) and stiff states (misaligned).

states of bonded laminates based on different layer alignments. Bonding between the individual layers is achieved using thin adhesive offsets (0.12 mm thickness) that are laminated with the outer layers under the hydraulic press (5000 psi for 30 s). The above fabrication steps are generic for building all types of aforementioned reconfigurable laminate designs.

Similar to any type of planar robot fabrication method, such a fabrication paradigm involves constant use of laser machining and manual assembling such as aligning and pressing of laminated layers. However, the method can work with a broad spectrum of materials such as metals, fibers, polymers, and fabrics, compared with a limited choice of workable materials as mostly seen in commercially available multi-material 3D printing technologies [56–58]. Due to the easy bonding of dissimilar materials through pressure-sensitive adhesives or even liquid adhesives a wide variety of materials can likely be used for reconfigurable laminates.

4. Results and discussions

4.1. Sliding-layer laminates enable variable stiffness building block

Reconfiguration of robot mechanical properties is highly desirable for adapting to changing locomotion challenges. Here we introduce sliding-layer laminates, which are based on the fabrication of multi-layered laminates that can slide relative to each other to form different alignment states that tune the passive bending stiffness of the entire bending structure. The concept can be implemented inside low-profile functional

structures, such as flapping appendages, with embedded actuation methods.

To characterize the potential for stiffness modulation with these structures we model sliding-layer laminates based on Euler–Bernoulli beam theory by calculating the cantilever beam bending stiffness and conduct experiments with different alignment states (figure 3). sliding-layer laminates are composed of repeatable stiffness patterns (e.g. rigid and soft), and thus we focus on the modelling and testing of a single laminate or beam unit, defined as one consecutive rigid and soft region. The governing equation for a beam's bending stiffness (linear regime) can be characterized by

$$\frac{\mathrm{d}^2 \omega(x)}{\mathrm{d}x^2} = \frac{M(x)}{E(x)I(x)} \tag{1}$$

where $\omega(x)$ is the incremental beam deflection at a horizontal beam location x. $M(x)$ is the bending moment exerted at the far end of the beam with $E(x)I(x)$ representing the flexural rigidity at individual beam location ($E(x)$, the Young's Modulus and $I(x)$, the second moment of area). Incremental beam deflections $\omega(x)$ can be integrated along the beam's length L for a total tip deflection ω as shown in (2).

$$\omega = \int_L \mathrm{d}\omega(x) = \iint_L \frac{M(x)}{E(x)I(x)} \mathrm{d}x^2. \tag{2}$$

The cantilever beam stiffness can thus be characterized in (3) based on the tip force.

$$k = \frac{F}{\omega} = \frac{F}{\iint_L \frac{M(x)}{E(x)I(x)} \mathrm{d}x^2}. \tag{3}$$

As the number of beams increases, modelling the combined beam stiffness can be converted as calculations of the integrated flexural rigidities at each longitudinal point of the beam as shown in figure 3(a). Note that the flexural rigidities from different components in a multilayer beam can simply be added together as the integrated flexural rigidities [59]. Therefore, we present a concept called the flexural rigidity matrix by listing out the rigidity components from one multilayer beam. We then integrate those into a 1D load carrier by summing up each rigidity component in a column wise fashion (figure 3(a)). The bending stiffness of the whole multilayer beam at different alignment states can thus be calculated based on their integrated flexural rigidities (see derivations in [18]).

The bending stiffness of the sliding-layer laminates is measured based on a fixed end cantilever beam test, as shown in figure 3(b). Here we focus on the stiffness characterization of a single beam unit (40 mm × 40 mm, 0.025 mm Kapton + 0.25 mm FR-4). All samples were linearly deflected by a load cell (100 g micro load cell, Phidgets) driven by a linear motorized stage. The effective bending stiffness was defined as the force reading divided by the recorded deflection. We then change the alignment state of the beam unit by incrementally sliding the central laminate to the designated distance and measure the corresponding stiffness as plotted in figure 3(c). As a parametric exploration, first we show

how geometric parameters will affect the stiffness-alignment curvature within one sliding-layer laminate unit. To proceed, we choose 'laminate aspect ratio' as the key geometric parameter defined as the length of the rigid region divided by the total length of one beam unit. As the alignment changes from −100% (fully aligned) to 0% (fully misaligned) to 100% (fully aligned again), a gradual increase and decrease of bending stiffness was observed from samples with a 60% laminate aspect ratio. Meanwhile, the stiffness change is more binary by having a 90% aspect ratio (longer rigid regions) with most of the alignment states displaying a high bending stiffness due to the long overlapping states of the rigid regions. Here we include rigid FR-4 linkages (4 mm in width) inside the soft regions of the central sliding-layer (40 mm × 36 mm) since completely Kapton-based soft regions are extremely compliant and will not generate enough force reading. Yet both cases exhibit significant stiffness variation between 3 (90%) and 7 (60%) folds. Note that the discrepancy between theoretical and experimental is largely caused by the imperfect physical contacts between dissimilar laminates which are often accompanied with nonlinear hinge buckling, that cannot be simply captured by linear beam theories. A further study is based on how material compositions (rigid and soft components), will affect the extreme stiffness states, namely the stiffest and softest states. As shown in figure 3(d), by incrementally increasing the flexural rigidity (2/5/8 mm FR-4 linkages, central layer, 90% aspect ratio) of the soft regions ($E_s I_s$), the stiffness of the laminates at the softest state (100% aligned) will also change linearly, with little influence on the stiffest state. A countering phenomenon was observed as we only vary the flexural rigidity (20/30/40 mm FR-4, all layers, 90% aspect ratio) of the rigid regions ($E_r I_r$). These studies provide insights for controlling the stiffness-alignment curvatures to be either gradual or binary, with the capability to vary the potential range of the tunable passive bending stiffness.

When the unit size of a sliding-layer laminate is small compared to the total beam length, the sliding-layer laminates can approximate a beam with continuous curvature and stiffness. We envision such stiffness changing continuum surfaces will have applications as robot appendages to interact with fluidic surroundings such as the wings and tails [60, 61]. In figure 4 we demonstrate such a concept by operating a 1D sliding-layer laminate design under different environments. In our first example, we mount a long sliding-layer beam (27 mm × 220 mm) inside a wind tunnel (wind speed: 8.5 m s^{-1}), whose alignment state is precisely controlled by a linear motorized stage (figures 4(a) and (b)). By changing the layer alignment, we are able to change the stiffness of the beam under constant wind conditions. We observe that altering the stiffness of the sliding-layer laminate beam induced or suppressed an aeroelastic fluttering behavior, highlighting a potential use for such stiffness tuning in sheets and beams. We tracked the tip amplitude of the beam as we altered the stiffness using a high-speed camera. In the soft state we observed a large amplitude flutter of the beam indicated by the tracked tip displacement, however when we change to the stiffest state the flutter is suppressed as indicated by small tip displacements (figure 4(c)). The beam stiffness
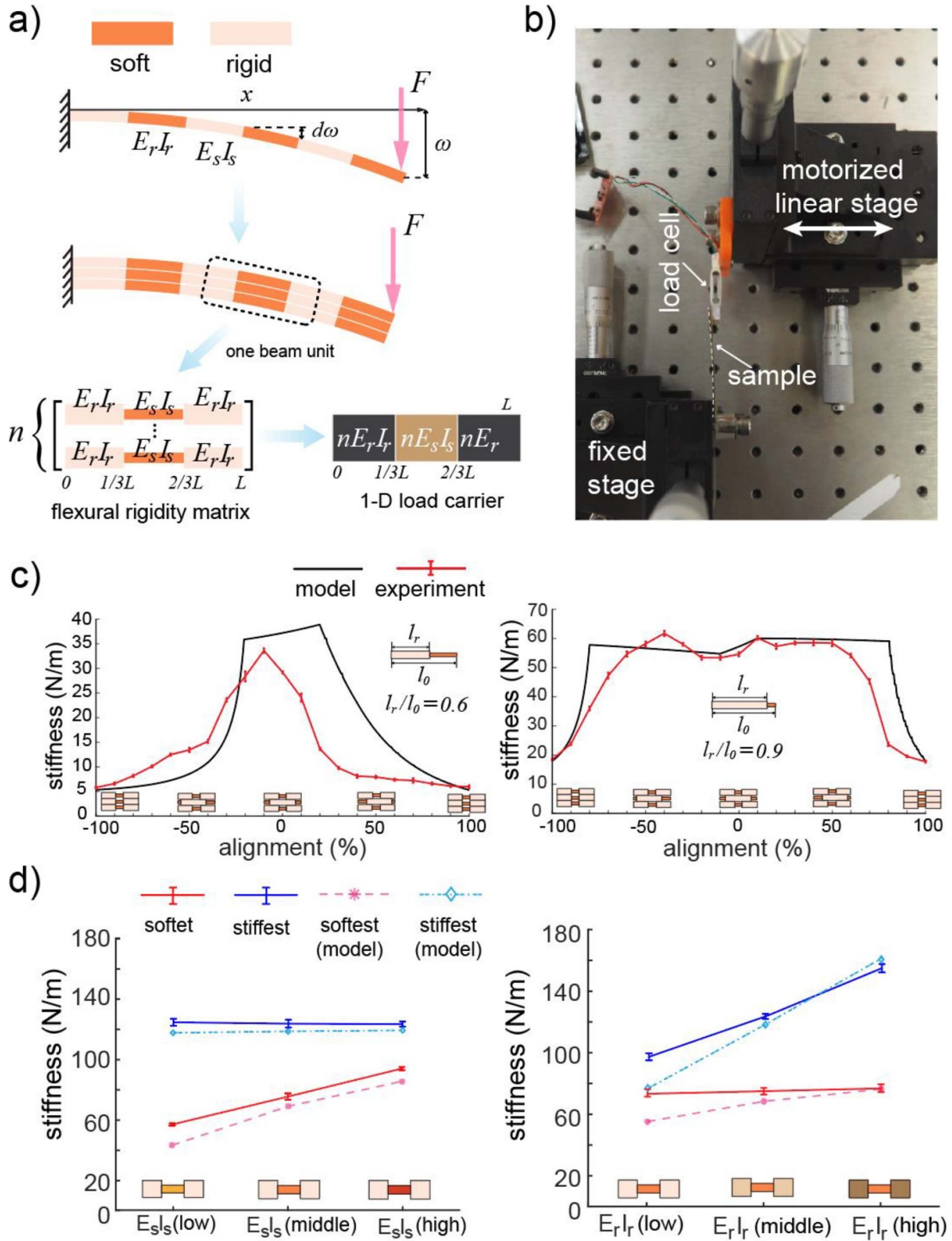
Figure 3. Results of sliding-layer laminates [18]. (a) Theoretical modelling of a multi-material multi-layered beam using Euler–Bernoulli beam theory. Stiffness profiles of each layer can be depicted using the flexural rigidities of each rigid and soft component, which can be combined as a one-dimensional (1D) load carrier. (b) Experimental setup for testing the bending stiffness of one sliding-layer laminate unit. (c) Variable bending stiffness measured over the entire sliding process with two laminate aspect ratios. The aspect ratio is defined as the length of the rigid region divided by the length of one complete beam unit. (d) Extreme stiffness states (stiffest and softest) measured from changing the material compositions of the rigid and soft components. Left: changing only the flexural rigidity of the soft components. Right: changing only the flexural rigidity of the rigid components. All results were averaged over five individual samples.
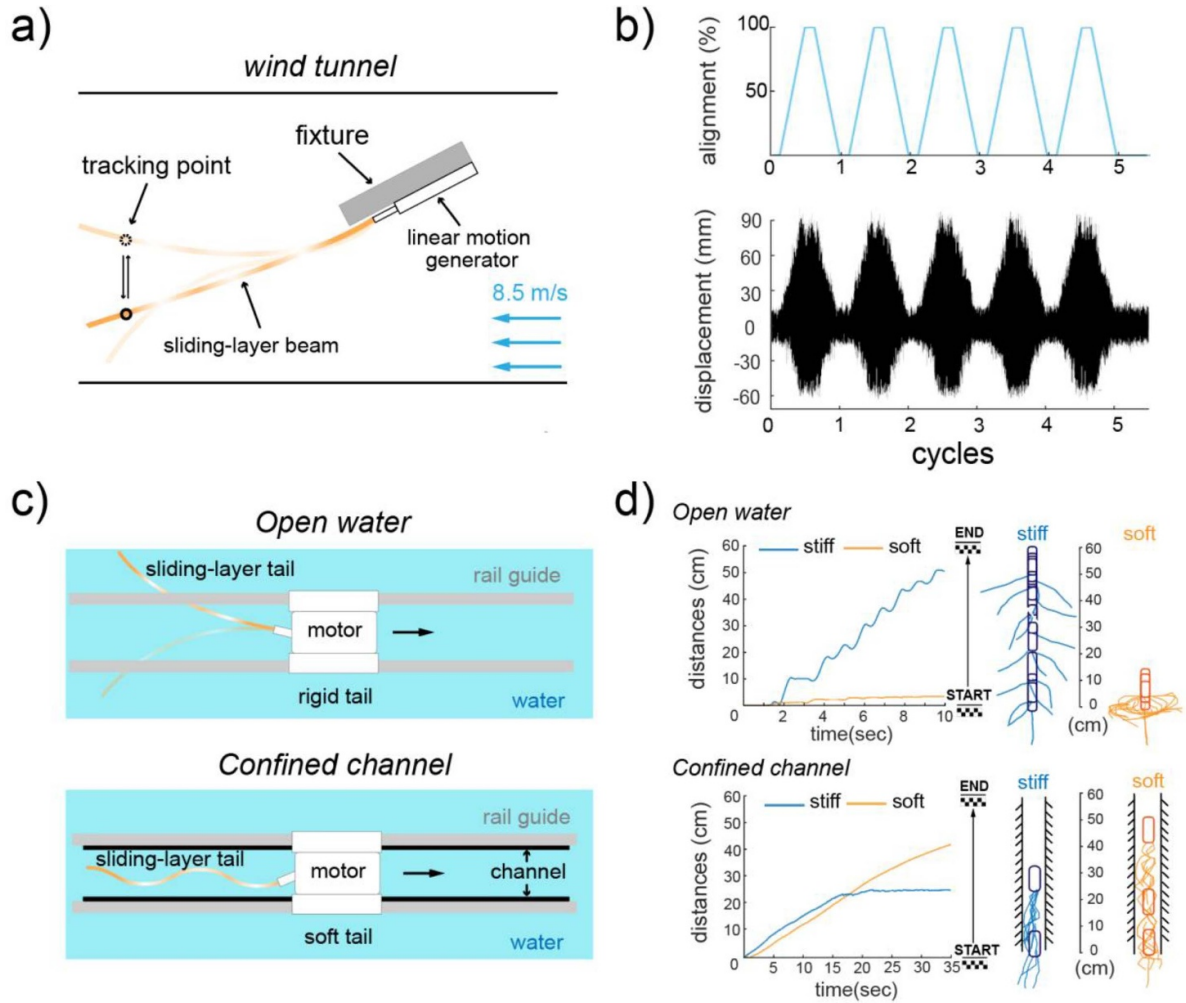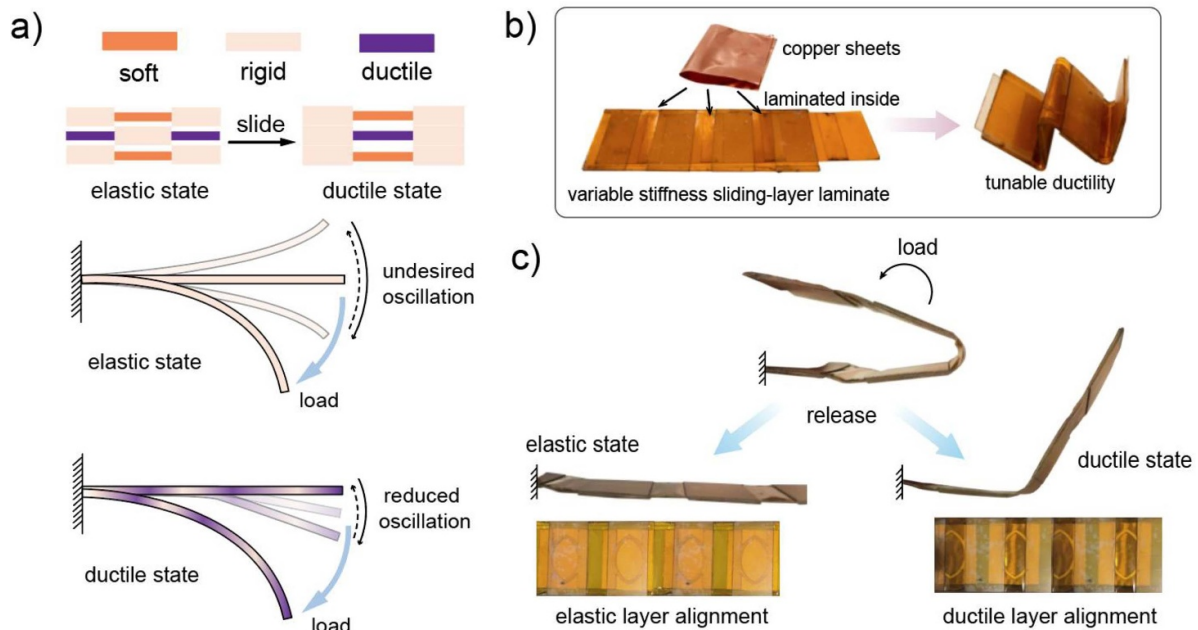
Figure 4. Demonstration of 1D sliding-layer laminates. (a) A variable stiffness beam fluttering inside a wind tunnel (wind speed: 8.5 m s^{-1}) with tunable tip displacements measured in the vertical direction (see supplementary video S1). The sliding layer was driven by a motorized linear stage. (b) The resulting tip flapping motion (vertical displacement) from the tunable layer alignment. (c) A robot with variable stiffness sliding-layer laminate-based fish tail operating under either open water or through a confined channel (see supplementary video S2). Switching of the tail stiffness was achieved via a solenoid linear actuator. (d) Swimming performances measured from different tail stiffness and working environments.

was tuned in a cyclic pattern to demonstrate the reversibility and repeatability of such a low-profile stiffness changing mechanism (see supplementary video S1 (available online at stacks.iop.org/SMS/30/035005/mmedia)). Future applications can involve stiffness modulation inside robotic appendages, such as variable stiffness flapping wing systems [62], for optimized aerodynamic performances, or as collapsible and recoverable wind turbines [63] for working under extreme conditions.

Our second example of sliding-layer laminates is in the application of an are also found useful to achieve underwater flapping tail systems to help robots navigate through confined and unconfined changeable underwater environments. In figure 4(d), we compare an underwater robot with variable stiffness flapping tail (45 mm × 260 mm) swimming under two different scenarios: open water and a confined channel and find that each case requires different tail stiffness for successful navigation. The tail was mounted onto a stepper motor that generates oscillatory motion and the motor is mounted on

a linear rail that allows for translation. The water tank was 20 cm deep and the channel was made from two acrylic sheets with a 45 mm channel width (figure 4(e)). In open water, the robot will gain more thrust by having its tail in the stiff state to generate more reaction force against the surrounding fluids with a large sweeping amplitude ($\pm72°$). However, as the robot enters a confined channel, the rigid tail causes physical interference with the channel entrance or undesired suction force against the channel wall preventing successful forward motion through the channel (figure 4(d)). In this case, switching the tail stiffness to its soft state permits the robot to navigate slowly but steadily through the channel with a smaller sweeping amplitude ($\pm21.6°$) (see supplementary video S2). The tail stiffness was switched based on the linear actuation of a solenoid (24 V, Guardian). The effective stroke distance of the solenoid is within 10 mm with a pulling force between 0.83 and 3.9 N. The solenoid was then rigidly coupled with one end of the central laminate for a direct change of the layer alignment. With a 10 mm stroke distance, the tail was able

Figure 5. Demonstration of 1D sliding-layer laminates with tunable ductility. (a) Diagrams showing the material composition of a ductile sliding-layer laminate with two states: elastic and ductile state. The ductile state will have reduced oscillation compared with the elastic state. (b) Fabrication of a tunable ductility sliding-layer laminate. (c) Upon releasing a loaded variable ductility laminate, the elastic state allows the beam to return to its neutral state with undesired oscillation, whereas the ductile state will be deformed to a certain degree with reduced oscillation (see supplementary video S3).

to change from the stiff to the soft state (soft hinge, 6 mm in the tail's lengthwise direction) quickly based on the input signal. The solenoid was also coupled with a linear spring, such that the tail will return back to its stiff state without further holding energy. Swimming performances for the two scenarios and two tail stiffness states are measured and shown in figure 4(f).

Mechanical reconfiguration generated by the sliding-layer laminates are not limited to varying just the elasticity of the beam. For instance, if we embed ductile materials such as copper sheets inside the soft hinged regions, a beam structure that can transition between elastic or ductile behavior can be created. The ability to tune the energy dissipation within the beam structure will significantly affect the damping ratio of the beam during static bending and oscillations (figures 5(a) and (b)). Figure 5(c) shows a laminated beam in its ductile state can be deformed into desired morphologies without external holding force, whereas its response against external loads exhibits increased damping that prevents the beam from undesired beam oscillations (supplementary video S3). While we present an example of this using a ductile material, any dissipative material can be embedded in the sliding-layer laminate for tunable mechanical energy dissipation.

As a final demonstration, we illustrate how sliding-layer laminates can be generated for two-dimensional sheet structures by creating stiffness patterns overlapping as cross-linkages along perpendicular axes (figure 6). Using the same sliding mechanism as in the beam examples, the two-dimensional sliding-layer laminate shows that such a sheet is capable of selectively changing its bending stiffness along individual axes and can be stiffened to resist load on the entire

surface as both axes are stiffened (figure 6 bottom row and supplementary video S4). Here the variable stiffness sheet structure is only demonstrated by a dual-axis sliding mechanism. However, stiffness changing with multi-axis can be achieved from more complex design patterns as long as each joint axis of the stiffness controllable directions align. The ability to generate two-dimensional stiffness changing laminates presents a wealth of opportunities for multi-functional laminate robot design.

4.2. Bi-stable reconfigurable joint via layer snapping

Sliding-layer laminates focus on how incremental adjustment of the layer alignment can uniformly change the mechanical properties of the entire beam (or sheet in the 2D case). In this section, we introduce reconfigurable joints, utilizing nonlinear thin-film buckling and snap through behaviors to enable bi-stable locking/unlocking of individual laminate joints within a reconfigurable laminate. A reconfigurable joint is composed of two laminate layers (top and bottom) with a horizontal misalignment of the rigid regions from the opposing layers (figure 7(a)). This creates pre-curved soft hinges as observed in the neutral (unlocked) state. When the joint is compressed, both hinges start to buckle outwards (pre-snapping) and continue to rotate as the layers are further displaced towards each other. As the buckled curvatures almost orient themselves towards the horizontal directions, one rigid plate starts to overlap with adjacent rigid plates and the soft hinges snap into the layer channel locking the joint. The hinge in the locked state is passively stable due to the surface friction formed by the buckled curvature (the
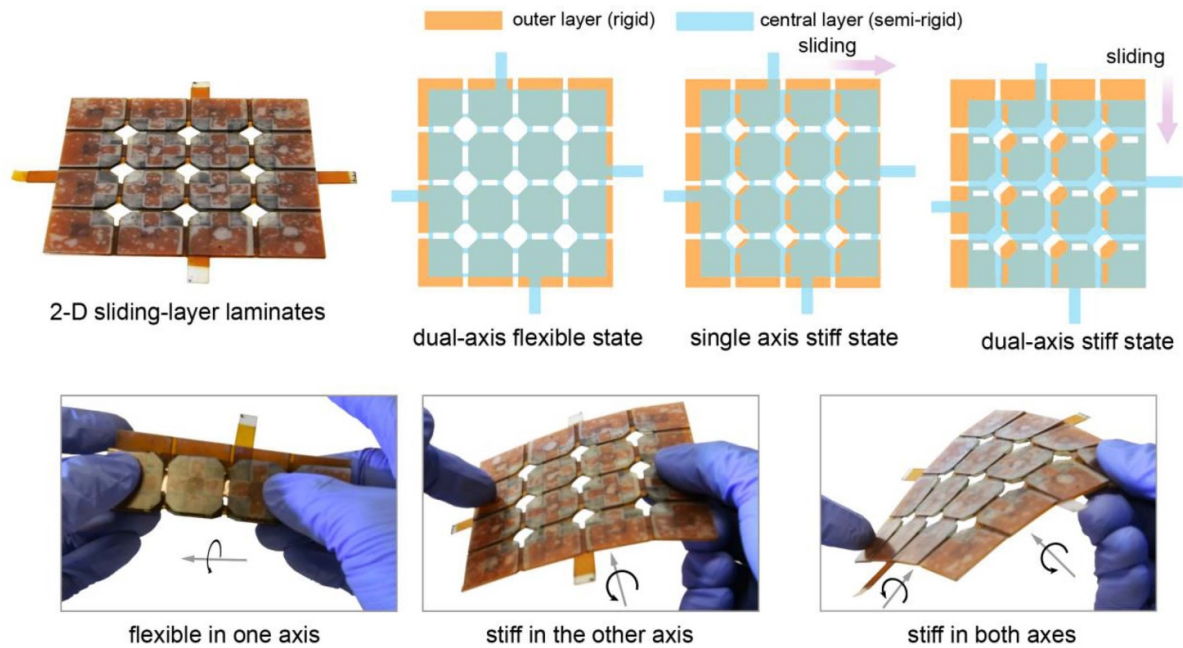
Figure 6. Demonstration of two-dimensional sliding-layer laminates in varying multi-axis bending stiffness of a sheet structure (see supplementary video S4).

'S' shape) as shown in figure 7(a). As the rigid components are stacked and overlapped inside the offset channel, the hinge will thus be stiffened to resist external loads. The principle of operations of the snapping hinge is shown in figure 7(a) and pictures from hands-on operations are shown in corresponding sequences in figure 7(b) (see supplementary video S5).

The ability for these joints to lock in place is provided by the intrinsic bistability of the buckled layer. To characterize the stability of the locked joint we studied push and pull force required to lock and unlock the joint. Here we fabricate reconfigurable joints (28 mm × 40 mm in total, 28 mm × 10 mm for soft hinge) with two different soft region thickness (0.025 mm and 0.05 mm, Kapton), where the rigid regions are made from fiberglass (FR-4, 0.25 mm). In the experiment, we secured one end of the beam units to a fixed location with the other end linearly actuated (push and pull) by a load cell mounted to a motorized linear stage (Thorlabs, MTS25-Z8, 25 mm) displaced at a 5 mm s^{-1} load speed (figure 7(c)). A 3D printed clamp was adapted with bolts and nuts to secure the connection between the load cell and the sample unit. As shown in figure 7(d), the joint locks itself with increasing external compressions due to the buckling of the soft hinges. As the buckled hinges rotate themselves and snap into the layer channel, the force drops until the snapped hinges are fully stored inside the layer channel. As the soft regions have already reached their final buckling states, further pushing will contribute to the overall compression of the beam unit, leading to an increased force as shown in the last bit of the locking process. During the unlocking process, force hysteresis is observed as the direction of the surface friction changes, leading to a pulling force to unlock the hinge. As shown in figure 7(d) left (0.05 mm Kapton), a

pulling force threshold is required to release the locked hinge. In experiments conducted on locking hinges with a thinner soft region (0.025 mm Kapton), a similar bi-stable push-pull loading force can be observed with significantly lowered locking and unlocking threshold compared to the previous experiments. Such a phenomenon can be explained by the increased buckling strength from thicker hinge components, whereas the nonlinear hysteresis between the locking and unlocking cycles are largely due to the nonlinear buckling behaviors as well as surface frictions from the inside-channel layer sliding motion. For each test, we start the load cell at the same starting location with the samples stretched by the same amount (by strains). The results plotted are averaged based on five individual locking/unlocking cycles per testing sample across five individual samples.

The stability of the locked-state in bi-stable joints and the ability to change individual joints presents several opportunities for reconfigurable mechanisms. For instance, locked reconfigurable joints can be utilized to hold curvatures in certain elastic structures, such as a buckling layer laminated on the outer side of the joint (figure 8(a)). An elastic buckling layer can thus be toggled to exhibit either buckling or flat state based on the input conditions of the snapping hinges. Here we assembled a laminate belt with passively sustainable curvature generated by the reconfigurable joints and the counter force provided by the elastic buckling layer (figure 8(a) middle). Hands-on operations of such a reconfigurable belt have been shown in figure 8(a) right, where the curved belt is capable of holding the curved shape passively (see supplementary video S6).

In addition to controlling individual joint stiffness, reconfigurable bi-stable joints can also be used to change the bending stiffness of laminated beam or sheet structures similar to
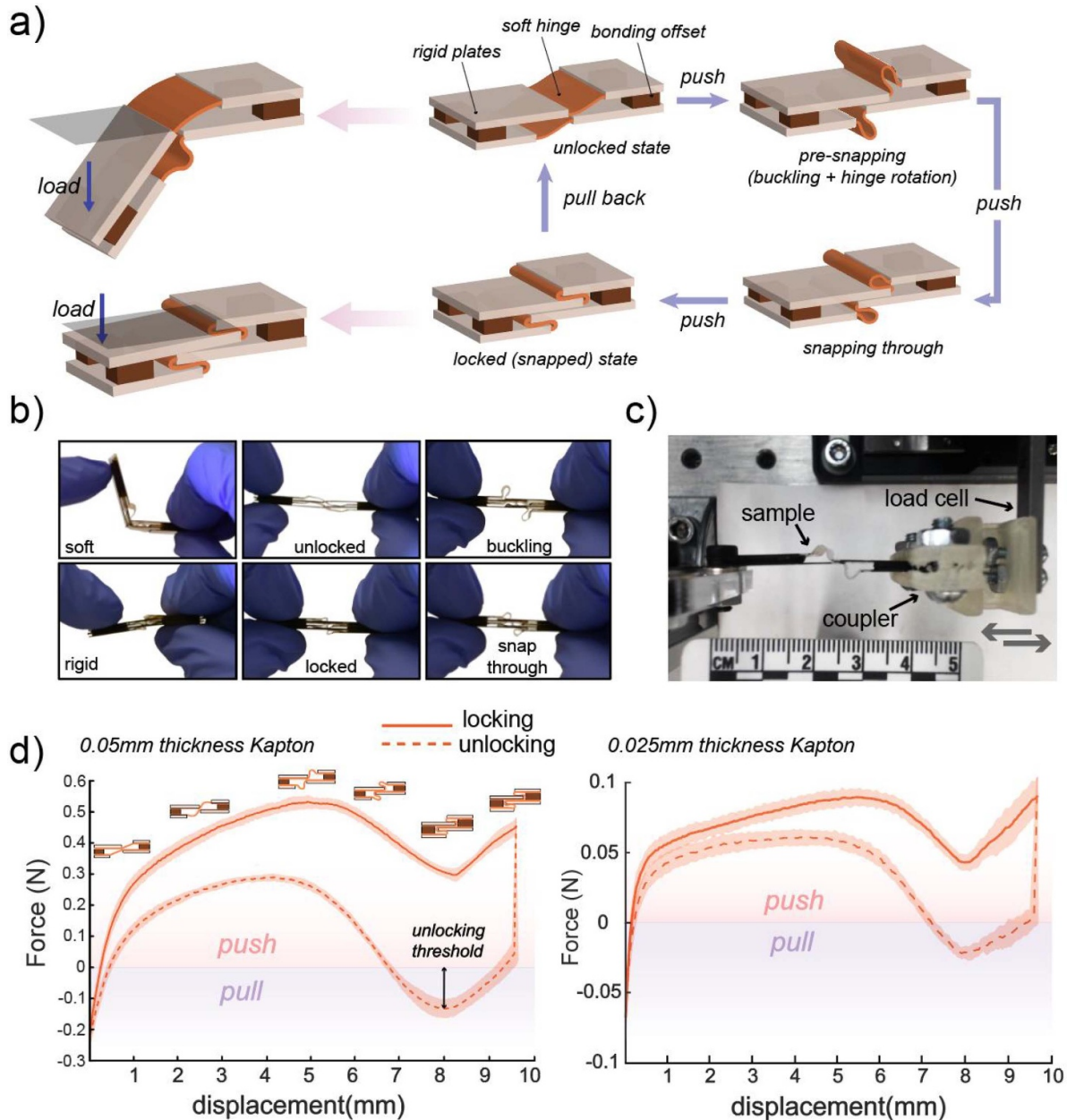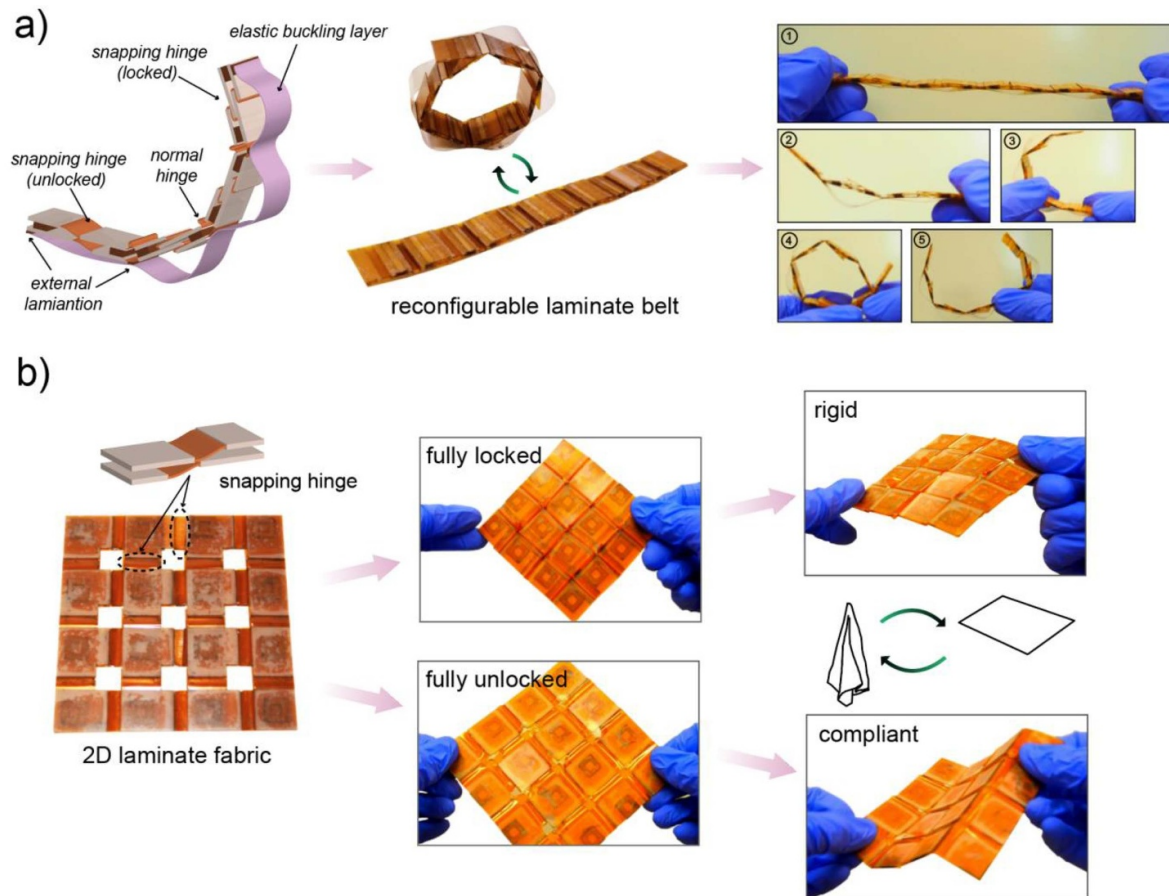
Figure 7. Illustration of reconfigurable joint mechanism and experimental results on the bistable joint activation forces. (a) Diagrams showing the principles of operation of a reconfigurable joint based on bistable snapping soft hinges. (b) A joint can thus be toggled to be rigid and soft based on simple push and pull actuations (see supplementary video S5). (c) Experimental setups for measuring the forces driving the snapping hinges during the lock unlocking cycles. (d) Force–displacement curvatures for driving the snapping hinges using a beam load cell (Futek, lbb200, 1lb max.) mounted on a motorized linear stage (Thorlabs, MTS25-Z8). The results are compared between two different material thickness of the soft regions, which are based on five individual testing samples for each case.

the capabilities of sliding-layer laminates. Arrays of bi-stable joints can be designed to hold an entire sheet or beam in a rigid or soft state. To demonstrate this capability, we built a two-dimensional laminate sheet, with bi-stable joints arrayed along an orthogonal pattern (figure 8(b)). By locking the bi-stable joints we are able to achieve an overall rigid state for the entire sheet. To unlock the entire array of bi-stable joints we simply apply tension along the two diagonal corners of the sheet and all hinges sequentially unlock leading to a fully compliant state similar to the 2D sliding-layer laminates (see supplementary video S7). However, unlike sliding-layer laminates where the

stiffness (compliance) can only be varied along an entire continuum structure or axis, reconfigurable joints allow for material stiffening and softening at local laminate joints and tiles. Currently, such a mechanism requires individual actuation of each reconfigurable joint which may add control difficulties as the degree of reconfigurability increases. However, embeddable actuations as well as control strategies such as multiplexing [64] by using only a few actuators could make it possible to achieve low-profile, multi-dimensional reconfigurable structures that change their local or global stiffness at will.

Figure 8. Demonstrations of reconfigurable materials from bi-stable snapping hinge reconfigurable joints. (a) A reconfigurable laminate belt with various self-sustainable curvatures (see supplementary video S6). (b) A variable stiffness two-dimensional laminate sheet achieved from arrays of bi-stable reconfigurable joints (see supplementary video S7).

4.3. Buckling-induced joint actuators

Previous sections have focused on the exploration of tunable mechanical and kinematic properties of reconfigurable laminate designs, such as tunable bending stiffness and joint creation. In this section, we introduce how laminate units can be actuated to generate directional bending based on the buckling state of the soft hinged regions. As shown in figure 9(a), we insert a tendon layer with no stiffness patterns inside the central channel. The tendon has an end stop placed at the far end of the laminate. To actuate the structure, we pull the tendon layer which applies compressive force on the soft hinges causing them to buckle and compress. Depending on the material compositions and thus buckling strength of the dual-layered soft region, either a joint contraction or bending motion can be achieved based on either symmetric or asymmetric buckling curvatures formed. A continuously bending structure (beam) can thus be formed by laminating serial joint actuators as shown in figure 9(a) right.

One unique aspect of the buckle-bend joint actuator is that even though the tendon layer is confined along the center of the layer channel, bending joint motion can still be generated by the asymmetric buckling and compressive elasticity of the top and bottom layers. Thus, the tendon does not require a

pre-offset lever arm for actuation and possibly can enable bi-directional actuation from a single one-ended tendon in future designs. The central tendon contributes to the overall thinness of the beam profile, and also allows for a high amplification ratio of the output motion based on a small input displacement. To demonstrate, we fabricated a bending actuator (160 mm × 24 mm × 4 mm) with the a large stiffness asymmetry of the soft regions; the top side was composed of thin Kapton (0.05 mm), and the bottom side was composed of thicker Mylar (0.1 mm). We recorded and tracked the tip trajectory of the actuator as shown in the dashed line (figure 9(b)). As the beam is linearly actuated, we recorded a 205° angular change $\Delta\theta_t$ from the tip of the beam with a distal-proximal travel distance, ΔL, of 167 mm based on a 10.5 mm tendon displacement, Δd (see supplementary video S8). Such a large amplification ratio (approximately 16:1) makes it possible to embed compact actuators with short stroke distances to generate a large bending actuation (tip angular change between 150° and 300°). As an example of using low-stroke actuation figure 9(c) shows a laminate bending actuator coupled with a McKibben actuator (33 mm length in total with 18% maximum contraction) to perform bending motions based on pneumatic input (see supplementary video S9). As further explorations, the laminate bending actuator was also programmed to
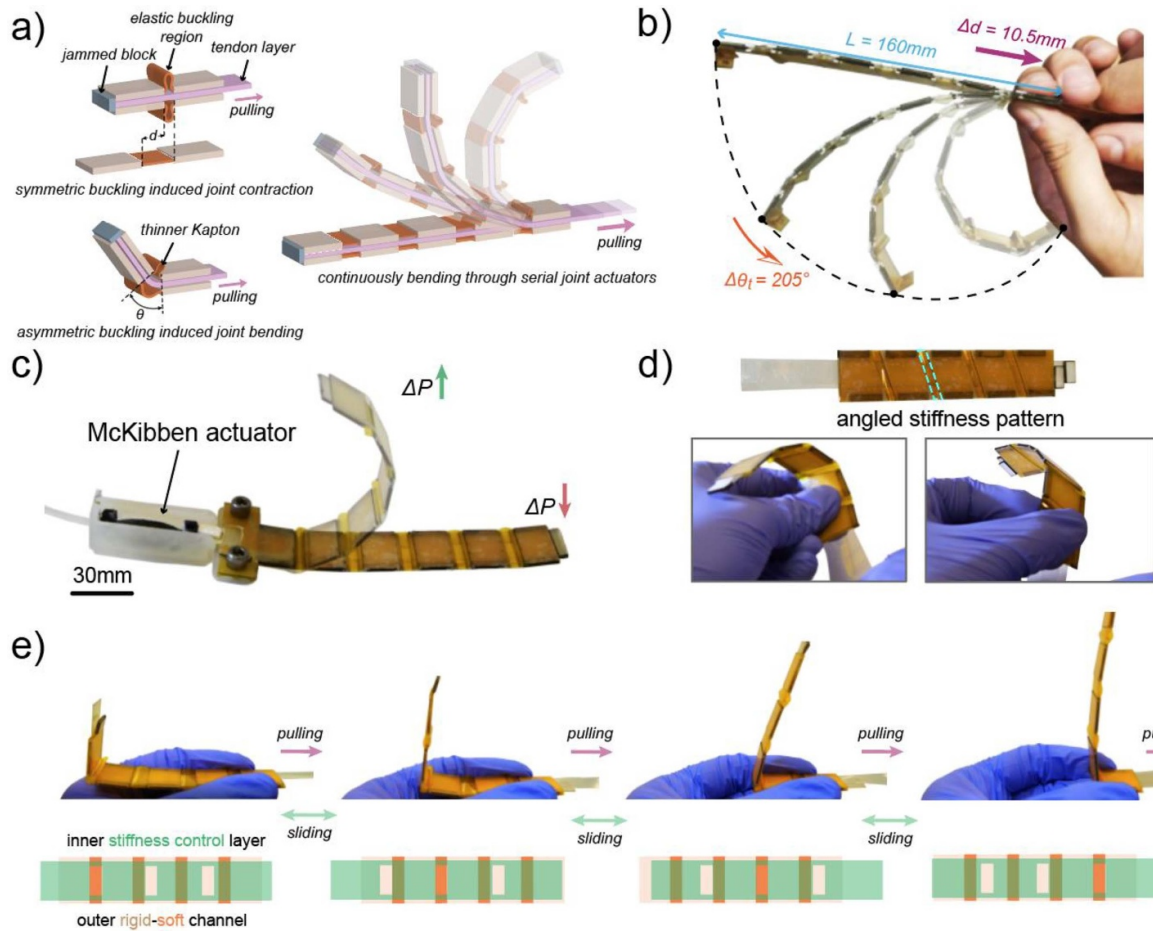
Figure 9. Buckle-bend joint actuators. (a) Design details of a buckle-bend joint actuator. Symmetric (top left) and asymmetric buckling (bottom left) from the dual-layered soft region enable extensional or bending actuation. (b) A time-lapse image of a bending beam actuated by a central tendon. Tip trajectory (dashed line) and bending parameters are shown. L—beam resting length, Δd—linear input and $\Delta \theta_t$—total angular displacement of the tip (see supplementary video S8). (c) An integrated bending actuator coupled with a pneumatic actuator (see supplementary video S9). (d) A bending actuator with out-of-plane bending motions controlled by angled stiffness patterns (see supplementary video S10). (e) Addressable actuation of each individual joint actuator by inserting a stiffness control layer based on tendon pulling (see supplementary video S11).

generate out-of-plane bending motions by having angled stiffness patterns on the soft hinged regions (figure 9(d), and supplementary video S10).

Thus far we have only used reconfigurability of the layers to displace a tendon for actuation. In this last section we combine the mechanical reconfigurability with the tendon actuation to create addressable joints of a multi-jointed structure using a single tendon. We incorporate a layer sliding mechanism into the buckle-bend joint actuators to selectively control the stiffness of individual joints. As shown in figure 9(e), a bending actuator composed of four individual joints can be sequentially actuated by reconfiguring a stiffness control layer that has appropriately aligned stiff and soft regions. By controlling the local stiffness of each actuator, a single actuation source can address individual joints (see supplementary video S11). Note that the sliding-layer may also include hybrid material components for achieving variable multi-material properties (e.g. stiffness and damping) of the bending actuator. Thus, incorporation of reconfigurable layer sliding can enable simultaneous control of actuation and stiffness state of reconfigurable

laminates. This presents new opportunities for building low-profile, multi-functional robotic bending actuators with integrated control of mechanical (joint stiffness and damping) and kinematic properties (addressable bending joints).

5. Conclusions

This paper presents a novel approach for building reconfigurable laminates to provide new multi-functional laminate-based structures for robotics. Compared with traditional rigid-flex laminate linkages that emulate single degree of freedom joint kinematics and dynamics, reconfigurable laminates are capable of modifying joint properties or location through sliding central layers. Reconfigurable laminates provide opportunities to vary the mechanical and kinematic properties of existing laminate structures without the requirements for constant energy supplies to hold any changed state; however, such designs pose a challenge for separate control and actuation of the added degrees of freedom based on the number of tunable

properties a system has. Future research should be focused on the incorporation of embeddable actuation methods such as shape-memory alloy, dielectric elastomer, or piezoelectric actuators. Embedded actuation would enable local control of the layer configuration and material properties and may even further expand the possibilities for reconfigurable robots made from such materials.

The design principles we present in this paper are not restricted to laminate based robotic structures. The ability to reconfigure joint morphology, mechanical stiffness, and other properties of a robot is a highly desirable feature for many robotics applications. The majority of the reconfiguration capabilities we demonstrate are due to the ability to reconfigure constituent materials that have heterogeneity. Thus, we propose that similar design principles can be applied to other fabrication processes that are capable of making heterogeneous materials such as multi-material 3D printing, shape deposition manufacturing, and multi-step 3D casting. We envision that reconfigurable robotic materials will enable new capabilities in soft robotics and that reconfigurable laminates provide a convenient palette of design capabilities for future exploration.

Acknowledgments

ORCID iDs

Mingsong Jiang ⬡ https://orcid.org/0000-0001-5414-872X
Nicholas Gravish ⬡ https://orcid.org/0000-0002-9391-2476

References

[1] Feczko J, Manka M, Krol P, Giergiel M, Uhl T and Pietrzyk A 2015 Review of the modular self reconfigurable robotic systems *2015 10th Int. Workshop on Robot Motion and Control* (*Romoco*) pp 182–7

[2] Miyashita S, Guitron S, Li S and Rus D 2017 Robotic metamorphosis by origami exoskeletons *Sci. Robot.* **2** eaao4369

[3] Xie H, Sun M, Fan X, Lin Z, Chen W, Wang L, Dong L and He Q 2019 Reconfigurable magnetic microrobot swarm: multimode transformation, locomotion, and manipulation *Sci. Robot.* **4** eaav8006

[4] Spröwitz A, Pouya S, Bonardi S, Den Kieboom J V, Möckel R, Billard A, Dillenbourg P and Ijspeert A J 2010 Roombots: reconfigurable robots for adaptive furniture *IEEE Comput. Intell. Mag.* **5** 20–32

[5] Firouzeh A, Sun Y, Lee H and Paik J 2013 Sensor and actuator integrated low-profile robotic origami *2013 IEEE/RSJ Int. Conf. on Intelligent Robots and Systems* pp 4937–44

[6] Hawkes E, An B, Benbernou N M, Tanaka H, Kim S, Demaine E D, Rus D and Wood R J 2010 Programmable matter by folding *Proc. Natl Acad. Sci. USA* **107** 12441–5

[7] Kotay K and Rus D 2005 Efficient locomotion for a self-reconfiguring robot *Proc. 2005 IEEE Int. Conf. on Robotics and Automation* pp 2963–9

[8] Kim J, Lee D, Kim S and Cho K 2015 A self-deployable origami structure with locking mechanism induced by buckling effect *2015 IEEE Int. Conf. on Robotics and Automation* (*ICRA*) pp 3166–71

[9] Li Y, Chen Y, Ren T and Hu Y 2018 Passive and active particle damping in soft robotic actuators *This work is funded by a basic research grant from the University of Hong Kong *2018 IEEE Int. Conf. on Robotics and Automation* (*ICRA*) pp 1547–52

[10] Kim H-S, Lee J-Y, Chu W-S and Ahn S-H 2017 Design and fabrication of soft morphing ray propulsor: undulator and oscillator *Soft Robot.* **4** 49–60

[11] Lee J-Y, Kang B B, Lee D-Y, Baek S-M, Kim W-B, Choi W-Y, Song J-R, Joo H-J, Park D and Cho K-J 2016 Development of a multi-functional soft robot (SNUMAX) and performance in robosoft grand challenge *Front. Robot. AI* **3** 63

[12] Wei Y, Chen Y, Ren T, Chen Q, Yan C, Yang Y and Li Y 2016 A novel, variable stiffness robotic gripper based on integrated soft actuating and particle jamming *Soft Robot.* **3** 134–43

[13] Shintake J, Schubert B, Rosset S, Shea H and Floreano D 2015 Variable stiffness actuator for soft robotics using dielectric elastomer and low-melting-point alloy *2015 IEEE/RSJ Int. Conf. on Intelligent Robots and Systems* (*IROS*) pp 1097–102

[14] Tolley M T, Felton S M, Miyashita S, Aukes D, Rus D and Wood R J 2014 Self-folding origami: shape memory composites activated by uniform heating *Smart Mater. Struct.* **23** 094006

[15] Okuzaki H, Saido T, Suzuki H, Hara Y and Yan H 2008 A biomorphic origami actuator fabricated by folding a conducting paper *J. Phys. Conf. Ser.* **127** 012001

[16] Xu T, Zhang J, Salehizadeh M, Onaizah O and Diller E 2019 Millimeter-scale flexible robots with programmable three-dimensional magnetization and motions *Sci. Robot.* **4** eaav4494

[17] Park Y-J, Lee J-G, Jeon S, Ahn H, Koh J, Ryu J, Cho M and Cho K-J 2016 Dual-stiffness structures with reconfiguring mechanism: design and investigation *J. Intell. Mater. Syst. Struct.* **27** 995–1010

[18] Jiang M and Gravish N 2018 Sliding-layer laminates: a robotic material enabling robust and adaptable undulatory locomotion *2018 IEEE/RSJ Int. Conf. on Intelligent Robots and Systems* (*IROS*) pp 5944–51

[19] Wood R J, Avadhanula S, Sahai R, Steltz E and Fearing R S 2008 Microrobot design using fiber reinforced composites *J. Mech. Des.* **130** 052304

[20] Wood R J, Avadhanula S, Menon M and Fearing R S 2003 Microrobotics using composite materials: the micromechanical flying insect thorax *2003 IEEE Int. Conf. on Robotics and Automation* (*Cat. No. 03CH37422*) vol 2 pp 1842–9

[21] Hoover A M and Fearing R S 2008 Fast scale prototyping for folded millirobots *2008 IEEE Int. Conf. on Robotics and Automation* pp 886–92

[22] Sreetharan P S, Whitney J P, Strauss M D and Wood R J 2012 Monolithic fabrication of millimeter-scale machines *J. Micromech. Microeng.* **22** 055027

[23] Zhakypov Z, Mori K, Hosoda K and Paik J 2019 Designing minimal and scalable insect-inspired multi-locomotion millirobots *Nature* **571** 381–6

[24] Mishra M K, Dubey V, Mishra P M and Khan I 2019 MEMS technology: a review *J. Eng. Res. Rep.* **4** 1–24

[25] Kim B J and Meng E 2015 Review of polymer MEMS micromachining *J. Micromech. Microeng.* **26** 013001

[26] Baisch A T and Wood R J 2013 Pop-up assembly of a quadrupedal ambulatory MicroRobot *2013 IEEE/RSJ Int. Conf. on Intelligent Robots and Systems* pp 1518–24

[27] McClintock H, Temel F Z, Doshi N, Koh J-S and Wood R J 2018 The milliDelta: a high-bandwidth, high-precision, millimeter-scale Delta robot *Sci. Robot.* **3** eaar3018

[28] Baisch A T, Ozcan O, Goldberg B, Ithier D and Wood R J 2014 High speed locomotion for a quadrupedal microrobot *Int. J. Robot. Res.* **33** 1063–82

[29] Onal C D, Tolley M T, Wood R J and Rus D 2015 Origami-inspired printed robots *IEEE/ASME Trans. Mechatron.* **20** 2214–21

[30] Chen Y, Ong A and Wood R J 2018 An efficient method for the design and fabrication of 2D laminate robotic structures *2018 IEEE Int. Conf. on Real-time Computing and Robotics* (*RCAR*) pp 19–24

[31] Cho K-J, Hawkes E, Quinn C and Wood R J 2008 Design, fabrication and analysis of a body-caudal fin propulsion system for a microrobotic fish *2008 IEEE Int. Conf. on Robotics and Automation* pp 706–11

[32] Jafferis N T, Helbling E F, Karpelson M and Wood R J 2019 Untethered flight of an insect-sized flapping-wing microscale aerial vehicle *Nature* **570** 491–5

[33] Hoffman K L and Wood R J 2011 Myriapod-like ambulation of a segmented microrobot *Auton. Robots* **31** 103

[34] Gafford J, Ranzani T, Russo S, Degirmenci A, Kesner S, Howe R, Wood R and Walsh C 2017 Toward medical devices with integrated mechanisms, sensors, and actuators via printed-circuit MEMS *J. Med. Device* **11** 011007

[35] Temel F Z, McClintock H, Payne C J, Wamala I, Walsh C J, Vasilyev N V and Wood R J 2017 Pop-up-inspired design of a septal anchor for a ventricular assist device *2017 Design of Medical Devices Conf.* (American Society of Mechanical Engineers Digital Collection)

[36] Wang L, Yang Y, Correa G, Karydis K and Fearing R S 2019 OpenRoACH: a durable open-source hexapedal platform with onboard robot operating system (ROS) *2019 Int. Conf. on Robotics and Automation* (*ICRA*) pp 9466–72

[37] Goldberg J D and Fearing R S 2015 Force sensing shell using a planar sensor for miniature legged robots *2015 IEEE/RSJ Int. Conf. on Intelligent Robots and Systems* (*IROS*) pp 1494–500

[38] Aukes D M, Goldberg B, Cutkosky M R and Wood R J 2014 An analytic framework for developing inherently-manufacturable pop-up laminate devices *Smart Mater. Struct.* **23** 094013

[39] Whitney J P, Sreetharan P S, Ma K Y and Wood R J 2011 Pop-up book MEMS *J. Micromech. Microeng.* **21** 115021

[40] Rus D and Tolley M T 2018 Design, fabrication and control of origami robots *Nat. Rev. Mater.* **3** 101–12

[41] Finio B M, Eum B, Oland C and Wood R J 2009 Asymmetric flapping for a robotic fly using a hybrid power-control actuator *2009 IEEE/RSJ Int. Conf. on Intelligent Robots and Systems* pp 2755–62

[42] Rus D and Tolley M T 2015 Design, fabrication and control of soft robots *Nature* **521** 467

[43] Kim S, Laschi C and Trimmer B 2013 Soft robotics: a bioinspired evolution in robotics *Trends Biotechnol.* **31** 287–94

[44] Tang Y, Chi Y, Sun J, Huang T-H, Maghsoudi O H, Spence A, Zhao J, Su H and Yin J 2020 Leveraging elastic instabilities for amplified performance: spine-inspired high-speed and high-force soft robots *Sci. Adv.* **6** eaaz6912

[45] Al Abeach L A T, Nefti-Meziani S and Davis S 2017 Design of a variable stiffness soft dexterous gripper *Soft Robot.* **4** 274–84

[46] Kim Y, Cheng S, Kim S and Iagnemma K 2013 A novel layer jamming mechanism with tunable stiffness capability for minimally invasive surgery *IEEE Trans. Robot.* **29** 1031–42

[47] Cheng N G, Lobovsky M B, Keating S J, Setapen A M, Gero K I, Hosoi A E and Iagnemma K D 2012 Design and analysis of a robust, low-cost, highly articulated manipulator enabled by jamming of granular media *2012 IEEE Int. Conf. on Robotics and Automation* pp 4328–33

[48] Chenal T P, Case J C, Paik J and Kramer R K 2014 Variable stiffness fabrics with embedded shape memory materials for wearable applications *2014 IEEE/RSJ Int. Conf. on Intelligent Robots and Systems* pp 2827–31

[49] Firouzeh A and Paik J 2015 Robogami: a fully integrated low-profile robotic origami *J. Mech. Robot.* **7** 021009

[50] Felton S, Tolley M, Demaine E, Rus D and Wood R 2014 A method for building self-folding machines *Science* **345** 644–6

[51] Mishra A K, Del Dottore E, Sadeghi A, Mondini A and Mazzolai B 2017 SIMBA: tendon-driven modular continuum arm with soft reconfigurable gripper *Front. Robot. AI* **4** 4

[52] Jeong S H, Kim K and Kim S 2016 Development of a robotic finger with an active dual-mode twisting actuation and a miniature tendon tension sensor *2016 IEEE Int. Conf. on Advanced Intelligent Mechatronics* (*AIM*) pp 1–6

[53] Cho K J, Hawkes E and Quinn C 2008 Design, fabrication and analysis of a body-caudal fin propulsion system for a microrobotic fish *2008 IEEE Int.*

[54] Jiang H, Li C and Huang X 2013 Actuators based on liquid crystalline elastomer materials *Nanoscale* **5** 5225–40

[55] Yang X, Shang W, Lu H, Liu Y, Yang L, Tan R, Wu X and Shen Y 2020 An agglutinate magnetic spray transforms inanimate objects into millirobots for biomedical applications *Sci. Robot.* **5** eabc8191

[56] Wallin T J, Pikul J and Shepherd R F 2018 3D printing of soft robotic systems *Nat. Rev. Mater.* **3** 84–100

[57] Jiang M, Zhou Z and Gravish N 2020 Flexoskeleton printing enables versatile fabrication of hybrid soft and rigid robots *Soft Robot.* **7** 770–8

[58] Bartlett N W, Tolley M T and Overvelde J T B 2015 A 3D-printed, functionally graded soft robot powered by combustion *Science* **349** 161–5

[59] Bareisis J 2006 Stiffness and strength of multilayer beams *J. Compos. Mater.* **40** 515–31

[60] McHenry M J, Pell C A and Long J H Jr 1995 Mechanical control of swimming speed: stiffness and axial wave form in undulating fish models *J. Exp. Biol.* **198** 2293–305

[61] Tytell E D, Leftwich M C, Hsu C-Y, Griffith B E, Cohen A H, Smits A J, Hamlet C and Fauci L J 2016 Role of body stiffness in undulatory swimming: insights from robotic and computational models *Phys. Rev. Fluids* **1** 073202

[62] Hale L, Patil M and Woolsey C 2012 Control of flapping wing micro-air vehicles using variable stiffness membrane wings *2012 American Control Conf.* (*ACC*) pp 2521–6

[63] Abu-Hamdeh N H and Almitani K H 2017 Construction and numerical analysis of a collapsible vertical axis wind turbine *Energy Convers. Manage.* **151** 400–13

[64] Bartlett N W, Becker K P and Wood R J 2020 A fluidic demultiplexer for controlling large arrays of soft actuators *Soft Matter* **16** 5871–7